View metadata, citation and similar papers at core.ac.uk
brought to you by CORE
provided by Lancaster E-Prints

Suppression of the surface "dead region" for fabrication of GaInAsSb thermophotovoltaic cells

Liangliang Tang[1], Qi Lu[2], Chang Xu[1], Andrew Marshall[2], Anthony Krier[2] and Zhuming Liu[3,*]

1. College of Energy and Electrical Engineering, Hohai University, Nanjing 210098, China

2. Quantum Technology Centre, Physics Department, Lancaster University, Lancaster, LA1 4YB, UK

3. Institute of Electrical Engineering, Chinese Academy of Sciences, Beijing 100190, China

***Corresponding Author:** Z. M. Liu, email:liuzhuming@mail.iee.ac.cn

Abstract

Zn diffusion processes in n-$Ga_{0.78}In_{0.22}As_{0.2}Sb_{0.8}$ epitaxial films are studied using different diffusion sources, a series of the Zn profiles with single and double humps are obtained. The group V-atoms (As and Sb) are found to have little effect on suppressing the surface "dead region". The Ga and In atoms have entirely different effect on diffusion although they are both group III-atoms. The "dead region" is suppressed completely under Ga-rich conditions, while the suppression will not occur under In-rich conditions. The GaInAsSb cells are fabricated under pure Zn and Ga-rich conditions. An electrical heating thermophotovoltaic system is fabricated for cell testing. Under the radiation from 1055℃-SiN ceramics emitter, the output power density of the GaInAsSb cell obtained under Ga-rich condition is much larger than that of the cell obtained under pure Zn condition, which demonstrated that the GaInAsSb cells can be fabricated without precise etching under Ga-rich conditions.

Keywords: Zn diffusion; GaInAsSb; thermophotovoltaic cells

1. Introduction

GaInAsSb is a quaternary compound semiconductor with a variable bandgap energy of 0.30~0.72eV when lattice-matched to a GaSb substrate [1]. GaInAsSb thermophotovoltaic (TPV) cells with a bandgap of 0.5~0.55eV have been fabricated [2-5] and are widely used in low-temperature (1000~1400K) TPV systems [6-9]. The power density of the state of art 0.55eV-GaInAsSb cell has reached the value of 0.34W/cm^2 under the 1073K-Silicon radiator [8].

Normally, epitaxial growth or a Zn diffusion process is used to form p-n junctions in GaInAsSb cells. An AlGaAsSb window layer should be deposited to reduce the high level of surface recombination if the epitaxial process is used [2, 3, 10]. However, cells with this type of structure are not suitable for near-field TPV systems owing to the surface window layer. The window layer is not needed for Zn-diffused cell structures, because the built-in electric field formed by the gradient in the Zn profile reduces the influence of the surface recombination. However, it is difficult to obtain the proper Zn profile in n-GaInAsSb for cell fabrication. A double-hump Zn profile is obtained when using Zn, Sb and InAs as the diffusion sources [5]. A kink point separates the two humps into heavily and lightly doped regions. The lifetime of photo-generated minority carriers is extremely short in the heavily doped regions, thus the first hump is usually called the "dead region", which needs to be removed by etching to enhance the performance of the cells.

Deviations are unavoidable between different batches of etching; therefore, it is difficult to precisely determine the etching depth for the kink point. Consequently, differences in the internal Zn profiles will result in the unstable cell performance. In this paper, we found that the first hump can be suppressed by controlling the diffusion sources, in which case the GaInAsSb cells can be fabricated without precise etching. The main idea of this paper comes from the novel Zn diffusion process for fabricating GaSb cells in our previous publication [11]. Furthermore, Zn diffusion in quaternary GaInAsSb are more complicated and interesting than that in binary GaSb. The remainder of this paper is organized as follows. Section 2 describes the Zn diffusion experimental procedures and results. Interesting diffusion phenomena are observed when using different diffusion sources. Section 3 gives the optimization of Zn-diffused emitter, and the GaInAsSb cells with different Zn profiles are fabricated and compared. Section 4 outlines the conclusions.

2. Zn diffusion in n-GaInAsSb

2.1. Experimental procedures for Zn diffusion

The tellurium doped, <100> oriented n-GaInAsSb ($n = 2\times10^{17}\,\mathrm{cm}^{-3}$ **)** epitaxial layers were grown on n-GaSb substrates by molecular beam epitaxy (MBE) at Lancaster University. The epitaxial thickness is 5 μm and the sample shows a mirrored surface after MBE growth. The bandgap energy of GaInAsSb we prepared is about 0.49eV from the photo-luminescence (PL) analysis. The

elemental composition is Ga: In: As: Sb=0.78: 0.22: 0.2: 0.8, which is got by combining X-ray diffraction fit with PL results.

Zn, Sb and InAs powders were previously used as diffusion sources and a double-hump Zn profile was obtained in n-GaInAsSb [5]. In order to distinguish the effect of the diffusion source, three types were chosen: pure Zn, Zn-As-Sb alloy (group V-atoms rich) and Zn-Ga-In alloy (group III-atoms rich). Both of the alloy sources contain 4wt% Zn and 48wt% of the other two elements. The alloy sources were prepared in vacuum at the temperature of 1000℃ for 10h. The purity of all elements used in the alloy sources is 99.9999%.

The carrier for wafers and diffusion sources is a pseudo-closed box made of quartz. The graphite box we used previously [12] is not chosen here because it can easily pollute the diffusion furnace. The carrier was placed in the center of a small sized OTF-1200X tube furnace. After the diffusion, the cooling fan of the diffusion furnace was opened automatically and the flow of protective gas was increased to further accelerate the cooling speed. Without delay, the flanges of the furnace were opened, and the carrier was removed and cooled in an Ar atmosphere to room temperature. The resulting Zn diffusion profiles in the n-GaInAsSb were obtained using a CAMECA IMS4F secondary ion mass spectrometer (SIMS).

2.2. Diffusion results under pure Zn and group V-atoms rich conditions

Fig. 1a shows the Zn profiles after diffusion under pure Zn conditions at 420~480℃ for 2h; a series of double-hump Zn profiles are obtained. The surface Zn concentration stays constant at about $2.3\times10^{20}\,cm^{-3}$ with increasing temperature, which is lower than the value of $4.5\times10^{20}\,cm^{-3}$ for n-GaSb [12, 13]. All the Zn profiles obtained under pure Zn conditions are not suitable for fabricating GaInAsSb cells directly because the lifetime of minority carriers is extremely short in the "dead region"; precise etching processes are necessary.

The group V-atoms are commonly added into the diffusion source during the Zn diffusion in binary III-V compound semiconductors [14-16]. Fig. 1b shows the Zn profiles in n-GaInAsSb after diffusion under As-Sb-rich at 420℃ for 2h, compared with the profile under pure Zn conditions. The As-Sb-rich diffusion yields similar results to that of the pure Zn diffusion sources. The depth of the "dead region" is shortened under As-Sb-rich conditions. Nevertheless, the precise etching process is still necessary for GaInAsSb TPV cell fabrication.

2.3. Diffusion results under group III-atoms rich conditions

The diffusion results are significantly different when Zn-Ga-In alloy sources are used. Fig. 2a shows the Zn profiles after diffusion annealing under Ga-In-rich conditions at 420~480℃ for 2h. The distorted phenomenon disappears, and all the Zn profiles show the single-hump shape. The surface Zn concentration is reduced by about one order and stays constant at $5\sim6\times10^{19}\,cm^{-3}$ with increasing temperature. Compared with the Zn profiles obtained under pure Zn or As-Sb-rich conditions, the first hump appears to be "removed" completely. The diffused emitters with single-hump Zn profiles are suitable for GaInAsSb cell fabrication; without etching process.

The Zn diffusion process in the quaternary GaInAsSb material is more complicated than in binary materials such as GaSb [13] and GaAs [17]. Although the "dead region" has been suppressed by using Zn-Ga-In sources, whether the Ga or In atoms are more important in the diffusion process remains unknown. The Zn (4wt%)-Ga and Zn (4wt%)-In alloy sources were prepared for further experiments.

Fig. 2b shows the Zn profiles in n-GaInAsSb after diffusion under Ga-rich and In-rich conditions at 420℃ for 2h, the Zn-Ga and Zn-In sources were used in the above two conditions. Large disparities were found between Ga-rich and In-rich conditions. Under the Ga-rich conditions, a single-hump Zn profile is obtained, similar to that for the Ga-In rich conditions. Conversely, a double-hump Zn profile is obtained under In-rich conditions, similar to that for the pure Zn conditions. The clear disparities demonstrate that the Ga atoms are effective in suppressing the formation of a "dead region".

Ga and In are both group III-atoms, so it is interesting that they have different effects on the Zn diffusion process. Inspired by the Caughey-Thomas model [18] for calculating electron and hole mobility from binary alloys, we processed several Zn diffusion experiments in binary alloys in order to seek the origin of the abnormal phenomenon in quaternary compound. The binary alloys of GaSb (78%), InAs (20%) and InSb (2%) constitute $Ga_{0.78}In_{0.22}As_{0.2}Sb_{0.8}$. The percentage of InSb is small, thus the Zn diffusions in GaSb and InAs are mainly considered.

Fig. 3a shows the Zn profiles in n-GaSb under pure Zn and Ga-rich conditions at 500℃ for 2h [11]. Large disparities can be found between the pure Zn and Ga-rich conditions, the Ga atoms from the diffusion source suppress the formation of the "dead region" completely. Fig. 3b shows the Zn

profiles in n-InAs under pure Zn and In-rich conditions at 440℃ for 2h. Single-hump Zn profiles are obtained under both conditions, and the surface Zn concentration is decreased under In-rich conditions. We found that the formation of the "dead region" in n-GaSb is caused by the self-diffusion of the Ga atoms from GaSb substrates [13], thus the In atoms cannot easily escape from InAs substrates because no "dead region" is formed even under pure Zn conditions. The above diffusion phenomenon in GaSb and InAs may explain the large disparities of Zn diffusion in n-GaInAsSb between Ga-rich and In-rich conditions.

2.4. Diffusion model and verification

Before establishing the diffusion model, the relationship between Zn diffusion coefficient (D) and Zn concentration (C) can be analyzed by using the Boltzmann-Matano method. Fig. 4a shows D as a function of C for typical single- and double-hump Zn profiles obtained under pure Zn and Ga-In-rich conditions at 420℃ for 2h. For the single-hump profile, the function of $D \propto C$ fits the main region (I), and $D \propto C^{-2}$ fits the near surface region (II). For the double-hump profile, the four regions are fitted as follows: $D \propto C$ for the second hump (I), $D \propto C^2$ for the dead region-first hump (III) and $D \propto C^{-2}$ for the short transition region (II). Region IV with the relation of $D \propto C^{-4}$ demonstrates the extremely shallow region that may be caused by the inaccuracy of SIMS testing or Zn vapor deposition. Other Zn profiles in n-GaInAsSb also show similar trends to those described above. For simplicity, a simulated $D \propto C$ profile fits the main region of a single-hump Zn profile or the second hump of a double-hump Zn profile, a simulated $D \propto C^2$ profile fits the first hump of a double-hump profile, as shown in Fig. 4b.

It is generally accepted that the dissociative [19] or kick-out [20] mechanism can be used to explain the Zn diffusion phenomenon in III-V compound semiconductors. The difference between them is whether Zn atoms move by occupying the group III vacancies or kicking out the group III atoms in the lattice. In view of the above Zn diffusion results, we can conclude that the dominating Zn diffusion mechanism is determined by the diffusion sources.

Under Ga-In-rich conditions, the native Ga vacancies in the surface region of GaInAsSb will be occupied by the Ga atoms from the diffusion sources, thus the escape of lattice-located Ga atoms will be suppressed. The lattice-located In atoms will not escape from the wafer surface no matter whether the In atoms are added into the sources or not. The Zn atoms can only move by kicking out Ga and In

atoms, thus the kick-out mechanism dominates. This process can be depicted as an interstitial Zn atom (Zn_i^+) kicking out a lattice-located Ga/In atom (Ga_{Ga}^0 / In_{In}^0) to the interstitial state (I_{Ga}^+ / I_{In}^+), after which the Zn atom will become an ionized acceptor (Zn_{Ga}^-) in the substitutional state (Zn_s^-) and a hole (h^+) will be produced:

$$Zn_i^+ + Ga_{Ga}^0 \rightarrow Zn_{Ga}^-(Zn_s^-) + I_{Ga}^+ + h^+ \quad (1a)$$

$$Zn_i^+ + In_{In}^0 \rightarrow Zn_{In}^-(Zn_s^-) + I_{In}^+ + h^+ \quad (1b)$$

According to our previously illustrated calculation method, the relationship of $D \propto C$ will be obtained from Equations 1a and1b. The simulated $D \propto C$ profile coincides well with the main regions of the single-hump Zn profile, as shown in Fig. 4b.

Under pure Zn conditions, a large number of Ga vacancies will be formed owing to the escape of Ga atoms from the wafer surface. Zn atoms will move by occupying the Ga vacancies in priority because it is easier to occupy the existing Ga vacancies than to kick out the lattice-located Ga or In atoms, thus dissociative diffusion will dominate in the first hump. This dissociative diffusion process can be depicted as an interstitial Zn atom (Zn_i^+) moving to occupy a Ga vacancy (V_{Ga}^0) and becoming an ionized acceptor (Zn_{Ga}^-); this reaction produces two holes (h^+):

$$Zn_i^+ + V_{Ga}^0 \rightarrow Zn_{Ga}^-(Zn_s^-) + 2h^+ \quad (2)$$

The relationship of $D \propto C^2$ can be obtained from Equation 2, and the simulated $D \propto C^2$ profile coincides well with the fist hump of the double-hump Zn profile, shown in Fig. 4b.

Since the Ga vacancies inside GaInAsSb are mainly generated by Ga escaping from the surface, with the deepening of diffusion, its concentration will decrease to a native equilibrium value. The lack of Ga vacancies will restrict further diffusion of Zn atoms by the dissociative mechanism. The interstitial Zn atoms will be forced to move by kicking out the lattice-located Ga or In atoms, thus the kick out mechanism dominates in the second hump of Zn profiles. The above deduction is verified by the nearly similar shape of the second hump of the double-hump Zn profile and the single-hump profile under the same diffusion temperature and duration, as shown in Fig. 4b.

In order to further verify the diffusion model, the Zn profiles obtained under pure Zn and Ga-In-rich conditions (Fig. 1a and 2a) are used to extract the diffusion parameters. The parameters of

surface concentration (C_{sur}) and surface diffusion coefficient (D_{sur}) can be extracted from the concentration-dependent diffusion process. The value of C_{sur} for the "dead region" of the double-hump Zn profiles stays nearly constant at $2.3\times10^{20}\,cm^{-3}$. The value of C_{sur} for the main region of the single-hump Zn profiles and the second hump of the double-hump Zn profiles stay nearly constant at $1.3\times10^{19}\,cm^{-3}$. Fig. 5a shows the Arrhenius plot of D_{sur} fitted for simulating the single and double-hump Zn profiles obtained at 420~480℃ for 2h. Arrhenius plots of D_{sur} show good linearity, i.e., the logarithmic values of D_{sur} are linear with the reciprocal values of diffusion temperature. The values of D_{sur} for the second hump of the double-hump Zn profiles are nearly equal to that of the main region of the single-hump Zn profiles. The above regularities demonstrate that our model provides a reasonable explanation for both types of Zn profiles and can be used to make accurate predictions under other diffusion conditions.

The above Zn diffusion model is suitable for guiding the diffusion process for fabricating GaInAsSb TPV cells. Additionally, we can make an approximate estimation for the diffusion depth because it is linear with the logarithm value of diffusion temperature (Fig. 5b). However, unsolved problems still exist for the mechanism analysis; the total value of D_{sur} is calculated for the kick-out mechanism, the proportion of Ga or In atoms which are kicked out to the interstitial state is still unknown; further studies will be focused on this issue.

3. Cell optimization and fabrication

3.1. Analysis of quantum efficiency for the GaInAsSb cells with different Zn profiles

The "dead region" in the emitter could be suppressed under Ga or Ga-In rich condition, which condition is better for cell fabrication is still unknown. Here we calculate the internal quantum efficiency (IQE) for GaInAsSb cells with different Zn profiles. Table 1 shows the basic parameters of GaInAsSb cells with Zn-diffused emitters used for simulation. The intrinsic carrier concentration n_i is calculated using the formula 1 in Ref. [18]. The hole and electron mobility can be interpolated using the formula A4 in Ref. [21], the relative data of binary alloys used for interpolating can be found in Ref. [10]. The other parameters in Tab. 1 are extracted from our experimental values.

The recombination parameters have a large selection range [4, 18, 22], different radiative (B) and Auger recombination coefficient (C_p and C_n) were used although the same composition of GaInAsSb was designed [4, 22]. The relatively high recombination values are chosen for simulation

in this paper, shown in Table 2. The photon recycling factor (φ) is set at 4 because a back surface reflector is not used. The Shokley-Read-Hall (SRH) lifetime ranges from 100 to 1000ns for GaInAsSb epitaxial layers of different qualities [4], and the value of 120ns is chosen for simulation. The interface recombination velocity between GaSb substrate and GaInAsSb epitaxial layer is set at 1500cm/s. The surface recombination velocity (S) for GaInAsSb is set at a high vaule of 10^6cm/s.

Table 1

Basic parameters of $Ga_{0.78}In_{0.22}As_{0.2}Sb_{0.8}$ cells with p-emitters at 300K used for simulation

Basic parameters	Numerical value
Intrinsic carrier concentration n_i, at 300K	$1.17\times10^{14}\,\mathrm{cm}^{-3}$
Absorption coefficient at 300K	$\alpha(E)=2.6\mu\mathrm{m}^{-1}\mathrm{eV}^{-0.5}(E-E_g)^{0.5}$
Antireflection layer: Si_3N_4 layer	0.20μm
Grid area/Surface area	6%
Thickness of N-GaSb substrate	500μm
Carrier concentration of N-GaSb substrate	$3\times10^{17}\,\mathrm{cm}^{-3}$
Thickness of N-$Ga_{0.84}In_{0.16}As_{0.14}Sb_{0.86}$ epitaxial layer	5μm
N- $Ga_{0.84}In_{0.16}As_{0.14}Sb_{0.86}$ doping: Te doping	$2\times10^{17}\,\mathrm{cm}^{-3}$
P-type emitter: Zn doping	Zn profile shows in Fig. 3b
Electron mobility in $Ga_{0.78}In_{0.22}As_{0.2}Sb_{0.8}$ at 300K $\mu=\mu_{\min}+\frac{\mu_{\max}-\mu_{\min}}{1+((N_D+N_A)/N_{\mathrm{ref}})^{\alpha}}$	$\mu_{\max}=7658\mathrm{cm}^2/\mathrm{V}\cdot\mathrm{s}$ $\mu_{\min}=1015\mathrm{cm}^2/\mathrm{V}\cdot\mathrm{s}$ $N_{\mathrm{ref}}=2.45\times10^{17}\,\mathrm{cm}^{-3}$ $\alpha=0.85$
Hole mobility in $Ga_{0.78}In_{0.22}As_{0.2}Sb_{0.8}$ at 300K $\mu=\mu_{\min}+\frac{\mu_{\max}-\mu_{\min}}{1+((N_D+N_A)/N_{\mathrm{ref}})^{\alpha}}$	$\mu_{\max}=742\mathrm{cm}^2/\mathrm{V}\cdot\mathrm{s}$ $\mu_{\min}=67\mathrm{cm}^2/\mathrm{V}\cdot\mathrm{s}$ $N_{\mathrm{ref}}=6.95\times10^{17}\,\mathrm{cm}^{-3}$ $\alpha=0.59$

Table 2

Summary of recombination parameters for $Ga_{0.78}In_{0.22}As_{0.2}Sb_{0.8}$ at 300K

Type	Recombination rates	Parameters
Radiative	$R_{Rad} = \frac{B}{\varphi}(np - n_i^2)$	$B = 1\times10^{-10}\,\mathrm{cm}^3/\mathrm{s} \quad \varphi = 4$
Auger	$R_{Aug} = (C_n + C_p p)(np - n_i^2)$	$C_p = C_n = 2\times10^{-28}\,\mathrm{cm}^6/\mathrm{s}$
Bulk SRH	$R_{SRH} = \frac{(np - n_i^2)}{\tau_{SRHe}(p + n_i) + \tau_{SRHh}(n + n_i)}$	$\tau_{SRHe} = \tau_{SRHh} = 120\mathrm{ns}$
Surface/Interface	$R_{Sur/Inter} = \frac{S_e S_h (np - n_i^2)}{S_e(p + n_i) + S_h(n + n_i)}$	Surface: $S_e = S_h = 10^6\,\mathrm{cm/s}$ Interface: $S_e = S_h = 1500\mathrm{cm/s}$

The GaInAsSb cells are simulated using 1-D numerical photovoltaic cell simulation program PC-1D. Fig. 6a shows the IQE of GaInAsSb cells with different Zn profiles at 300K. Under pure Zn or In rich diffusion conditions, the double-hump Zn profile with a surface "dead region" is obtained, thus the IQE of the cell is low, especially in the surface region. Under Ga or Ga-In rich diffusion conditions, the surface "dead region" is suppressed, the IQE of the cell increases obviously. Although the IQE of the cell obtained under Ga-rich condition is lower than that for Ga-In-rich conditions in the short-wave bands, the IQE is larger than the latter in the long-wave bands after 1000nm, which is suitable for TPV systems. The IQE of GaInAsSb cell will decrease rapidly if the uniform doped emitter is designed and a window layer should be deposited to reduce to *S* value [2, 10]. Our calculation shows that the IQE of the cell without a window layer keeps at a high value, which is benefit from the strong built-in electrical fields generated by the gradient doping [5]. With a 0.20 μm Si_3N_4 anti-reflection (ARC) layer, the external quantum efficiency (EQE) and reflectivity (REF) for the cell obtained under Ga-rich condition are calculated, shown in Fig. 6b.

3.2. Cell fabrication and testing

The GaInAsSb cell samples were fabricated using Zn diffusion method, Fig. 7 shows the fabrication process and cell samples. Firstly, a 5 μm n-GaInAsSb exptaxial layer was grown on the n-GaSb surface by MBE. By padding a metal mask in the central, an insulating layer of SiO with a thickness of approximately 0.15 μm was evaporated on the border of the upper surface. Zn diffusion

process was used to form pn junctions, both the Ga and pure Zn diffusion conditions were used for comparison. After etching of backside diffusion layers, Ti/Pt/Au layers were deposited for back electrode and Pt/Au layers for the front electrode. The pattern of the front-side electrodes were defined through a hollowed-out metal mask. The front electrode has 60 μm -wide grids with 940 μm -wide spacing. Finally, a 0.20- μm -thick layer of Si_3N_4 film was deposited on the cell surface as an ARC coating.

A simple electrical heating TPV system was designed for output testing, shown in Fig. 8. The GaInAsSb cell was mounted on a water cooling apparatus made of copper (Fig. 8b). A custom-made silicon nitride (SiN) ceramic heater with a width of 30mm was used as an infrared (IR) emitter (Fig. 8c, d). The expected design temperature was 1100℃, and an actual highest temperature in the centre of the IR emitter reached about 1055℃. An electrode load was used for changing the circuit current.

Table 3. The output performance of GaInAsSb cells at the radiation temperature of 1055℃.

Data sources	Cell type	Radiator type	I_{sc}(A/cm^2)	V_{oc} (V)	Fill facter	P_{max} (W/cm^2)
Experiments	Cell 1	SiN ceramics	2.170	0.231	0.469	0.235
	Cell 2	SiN ceramics	1.042	0.187	0.441	0.086
Calculations	Cell 1	Given-blackbody	8.815	0.240	0.549	1.163
	Cell 2	Given-blackbody	6.895	0.208	0.513	0.737

Figure 9 and Table 3 show the output performance of GaInAsSb cells at the radiation temperature of 1055℃. Cell 1and 2 represent the cells obtained under Ga-rich and pure Zn conditions, respectively. Under the radiation from 1055℃-SiN ceramics emitter, the maximum power output density (P_{max}) of the cell 1 reaches 0.235W/cm^2, which is much better than cell 2. The bandgap of $Ga_{0.78}In_{0.22}As_{0.2}Sb_{0.8}$ is 0.49eV, this is the lowest value so far, and thus the cell has a relatively low open-circuit voltage (V_{oc}). The output performance of cells are calculated under 1055℃ -given-blackbody radiation using the EQE data in Fig. 6b. The short-circuit current (I_{sc}) under given-blackbody radiation is much larger than the experimental values under the SiN ceramics emitters. The emissivity of SiN ceramics with a smooth surface is about 0.85 in the wave range of 0.4~5 μm [23, 24], therefore, the efficiency of our fabricated GaInAsSb cell is less than 2% under the

1055℃-SiN ceramic emitter. This low efficiency might be affected by the front sparse electrode grids and the cell temperature increasing under actual working conditions. Moreover, good-quality IR emitters with effective filters should be developed to enhance the cell efficiency in the future. The experimentally evaluated performance of Cell 2 seems very low. The power degradation speed is faster than the calculation values. The quality deterioration of the GaInAsSb epitaxial layer might happen during pure Zn diffusion conditions due to the escaping of lattice-located Ga atoms, and this quality deterioration might account for the disparity of calculation and experimental degradation values.

4. Conclusions

In conclusion, the "dead region" up to the first hump of Zn profiles in n-GaInAsSb can be suppressed when using Zn-Ga-In or Zn-Ga alloy sources; so that the GaInAsSb TPV cells can be subsequently fabricated without precise etching. The escape of Ga atoms from the GaInAsSb surface is the origin of the "dead region". The In atoms were found to have little effect on Zn diffusion because the In atoms are relatively stable in the lattice of GaInAsSb. The IQE of GaInAsSb cells with different Zn profiles are analyzed, and Ga-rich condition is found to be fit for cell fabrication. Cell samples are fabricated and tested under 1055℃-SiN ceramics emitter, the output density of the cell obtained under Ga-rich condition is much larger than that obtained under pure Zn condition, which verified that the GaInAsSb cells can be fabricated without precise surface etching.

The output power density of our fabricated GaInAsSb cell is still low. The reasons for this low density mainly include the sparse front electrode defined by hollow-out metal mask and the simple IR source fabricated by SiN ceramics. Further studies will be focused on the above issues to increase the output power density of GaInAsSb cells.

Acknowledgment

This work was supported in part by the National Natural Science Foundation of China (No. 51506045) and in part by the Natural Science Foundation of Jiang Su (No. BK20150805).

References:

[1] R. Magri, A. Zunger, H. Kroemer, Evolution of the band-gap and band-edge energies of the lattice-matched

GaInAsSb/GaSb and GaInAsSb/InAs alloys as a function of composition, J. Appl. Phys. 98 (2005) 043701.
[2] H. Choi, C. Wang, G. Turner, M. Manfra, D. Spears, G. Charache, L. Danielson, D. Depoy, High-performance GaInAsSb thermophotovoltaic devices with an AlGaAsSb window, Appl. Phys. Lett. 71 (1997) 3758-3760.
[3] C. Wang, H. Choi, S. Ransom, G. Charache, L. Danielson, D. DePoy, High-quantum-efficiency 0.5 eV GaInAsSb/GaSb thermophotovoltaic devices, Appl. Phys. Lett. 75 (1999) 1305-1307.
[4] M.W. Dashiell, J.F. Beausang, H. Ehsani, G. Nichols, D.M. Depoy, L.R. Danielson, P. Talamo, K.D. Rahner, E.J. Brown, S.R. Burger, Quaternary InGaAsSb thermophotovoltaic diodes, IEEE T. Electron Dev. 53 (2006) 2879-2891.
[5] O. Sulima, R. Beckert, A. Bett, J. Cox, M. Mauk, InGaAsSb photovoltaic cells with enhanced open-circuit voltage, IEE Proc. -Optoelectron. 147 (2000) 199-204.
[6] K. Qiu, A. Hayden, M. Mauk, O. Sulima, Generation of electricity using InGaAsSb and GaSb TPV cells in combustion-driven radiant sources, Sol. Energy Mater. Sol. Cells 90 (2006) 68-81.
[7] K. Qiu, A. Hayden, Direct thermal to electrical energy conversion using very low bandgap TPV cells in a gas-fired furnace system, Energ. Convers. Manage. 79 (2014) 54-58.
[8] W.R. Chan, P. Bermel, R.C. Pilawa-Podgurski, C.H. Marton, K.F. Jensen, J.J. Senkevich, J.D. Joannopoulos, M. Soljačić, I. Celanovic, Toward high-energy-density, high-efficiency, and moderate-temperature chip-scale thermophotovoltaics, Pro. Nat. Acad. Sci. USA 110 (2013) 5309-5314.
[9] O.V. Sulima, A.W. Bett, M.G. Mauk, F. Dimroth, P.S. Dutta, R.L. Mueller, GaSb-, InGaAsSb-, InGaSb-, InAsSbP- and Ge-TPV cells for low-temperature TPV applications, in: Proceedings of the Fifth Conference on Thermophotovoltaic Generation of Electricity, Rome, 2003, pp. 434-441.
[10] X. Peng, X. Guo, B. Zhang, X. Li, X. Zhao, X. Dong, W. Zheng, G. Du, Numerical analysis of the short-circuit current density in GaInAsSb thermophotovoltaic diodes, Infr. Phys. Technol. 52 (2009) 152-157.
[11] L. Tang, H. Ye, J. Xu, A novel zinc diffusion process for the fabrication of high-performance GaSb thermophotovoltaic cells, Sol. Energy Mater. Sol. Cells 122 (2014) 94-98.
[12] H. Ye, L. Tang, Y. Ma, Experimental and theoretical investigation of zinc diffusion in N-GaSb, Chinese Sci. Bull. 55 (2010) 2489-2496.
[13] H. Ye, L. Tang, K. Li, The intrinsic relationship between the kink-and-tail and box-shaped zinc diffusion profiles in n-GaSb, Semicond. Sci. Tech. 28 (2013) 015001-1-015001-6.
[14] A.W. Bett, S. Keser, O.V. Sulima, Study of Zn diffusion into GaSb from the vapour and liquid phase, J. Cryst. Growth 181 (1997) 9-16.
[15] N.H. Ky, L. Pavesi, D. Araujo, J. Ganiere, F. Reinhart, A model for the Zn diffusion in GaAs by a photoluminescence study, J. Appl. Phys. 69 (1991) 7585-7593.
[16] S. Reynolds, D.W. Vook, J.F. Gibbons, Open-tube Zn diffusion in GaAs using diethylzinc and trimethylarsenic: Experiment and model, J. Appl. Phys. 63 (1988) 1052-1059.
[17] H. Ye, L. Tang, Q. Ni, Identification of the dissociative and kick-out diffusion mechanisms of Zn diffusion in GaAs by photoluminescence analysis, Mat. Sci. Eng. B 197 (2015) 1-4.
[18] X. Peng, B. Zhang, G. Li, J. Zou, Z. Zhu, Z. Cai, S. Zhou, Y. Li, Z. Wang, W. Jiang, Simulation of temperature-dependent material parameters and device performances for GaInAsSb thermophotovoltaic cell, Infrared Phys. Techn. 54 (2011) 454-459.
[19] B. Tuck, M.A.H. Kadhim, Anomalous diffusion profiles of zinc in GaAs, J. Mater. Sci. 7 (1972) 585-591.
[20] U. Gösele, F. Morehead, Diffusion of zinc in gallium arsenide: A new model, J. Appl. Phys. 52 (1981) 4617-4619.
[21] A. Krier, Mid-infrared Semiconductor Optoelectronics, Springer press, Germany, 2006.
[22] W. Yu, Y.Y. Lou, Radiant thermal conversion in 0.53eV GaInAsSb thermophotovoltaic diode, Renew. Energy.

75 (2015) 8-13.
[23] K. Yu, Y. F. Liu, Y. J. Zhao, Review of normal spectral emissivity standard reference materials, Spectrosc. Spectral Anal. 32 (2012) 2911-2915.
[24] Q. Cheng, P. Yang, Z. Zhang, Radiative Properties of Ceramic Al_2O_3, AlN, and Si_3N_4: I. Experiments, Int. J. Thermophys. 37 (2016) 1-16.

Fig. 1. The Zn profiles in n-GaInAsSb after diffusion under different diffusion sources. (a) Pure Zn conditions. (b) As-Sb-rich conditions and comparisons.

Fig. 2. The Zn profiles in n-GaInAsSb after diffusion under different diffusion sources. (a) Ga-In-rich conditions. (b) Ga-rich and In-rich conditions and comparisons.

Fig. 3. Comparison of Zn diffusion results in GaSb and InAs. (a) The Zn profiles in n-GaSb under pure Zn and Ga-rich conditions. (b) The Zn profiles in n-InAs under pure Zn and In-rich conditions.

Fig. 4. (a) Zn diffusion coefficient as a function of concentration for typical single and double hump Zn profiles. (b) Simulations for the single and double-hump Zn profiles.

Fig. 5. (a) Arrhenius plot of D_{sur} fitted for simulating the single and double hump Zn profiles obtained at 420~480℃ for 2h. (b) Diffusion depth and kink depth for Zn profiles in Fig. 1a and 2a.

Fig. 6. (a) Simulated IQE of GaInAsSb cells with different Zn profiles at 300K. (b) Simulated IQE, EQE and REF of the cell obtained under Ga-rich condition.

Fig. 7. GaInAsSb cell fabrication process using Zn diffusion method and cell samples.

Fig. 8. A simple electrical heating TPV system used for output testing. (a) An overview; (b) A water cooling apparatus for cell mounting. (c) SiN ceramic emitter before and (d) after heated.

Fig. 9. The I-V curve and power output density of GaInAsSb cells under (a) 1055℃-SiN ceramic emitter and (b) 1055℃-given blackbody radiations.

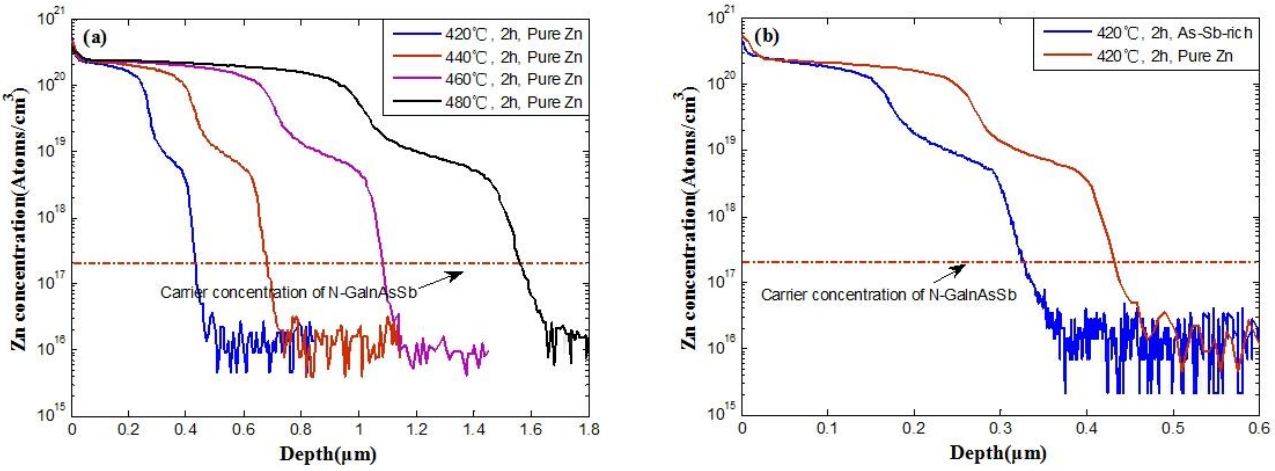

Fig. 1. The Zn profiles in n-GaInAsSb after diffusion under different diffusion sources. (a) Pure Zn conditions. (b) As-Sb-rich conditions and comparisons.

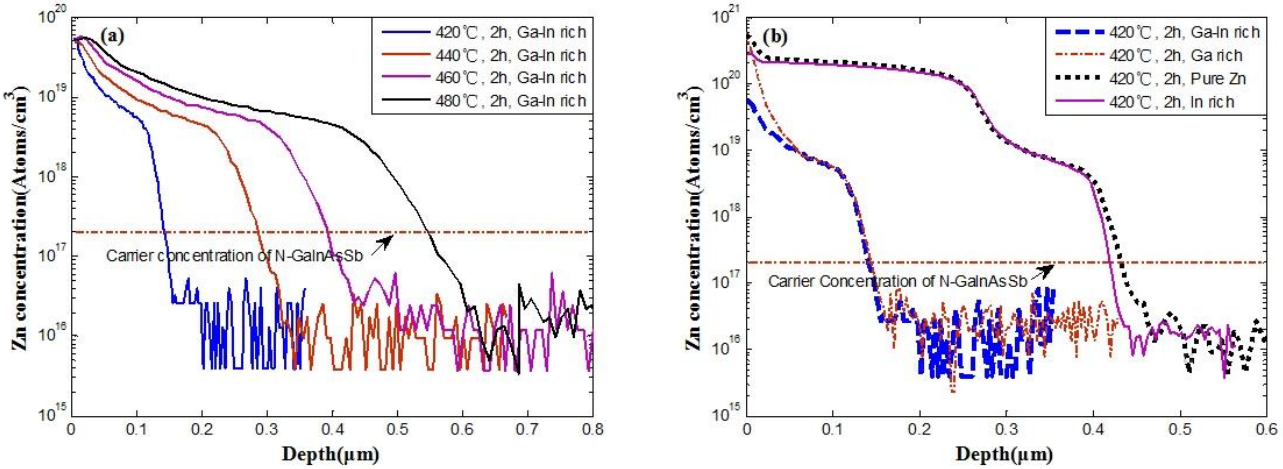

Fig. 2. The Zn profiles in n-GaInAsSb after diffusion under different diffusion sources. (a) Ga-In-rich conditions. (b) Ga-rich and In-rich conditions and comparisons.

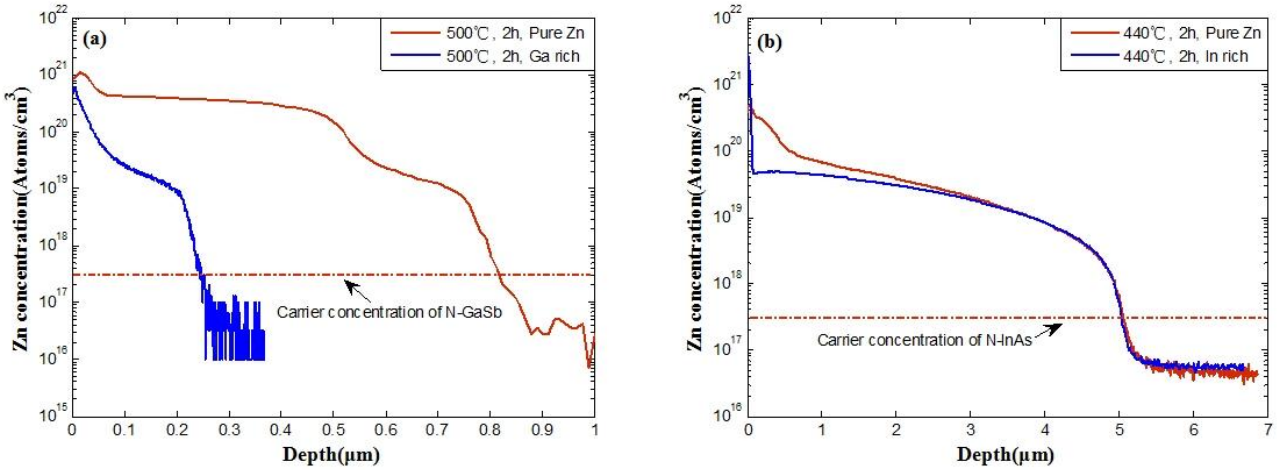

Fig. 3. Comparison of Zn diffusion results in GaSb and InAs. (a) The Zn profiles in n-GaSb under pure Zn and Ga-rich conditions. (b) The Zn profiles in n-InAs under pure Zn and In-rich conditions.

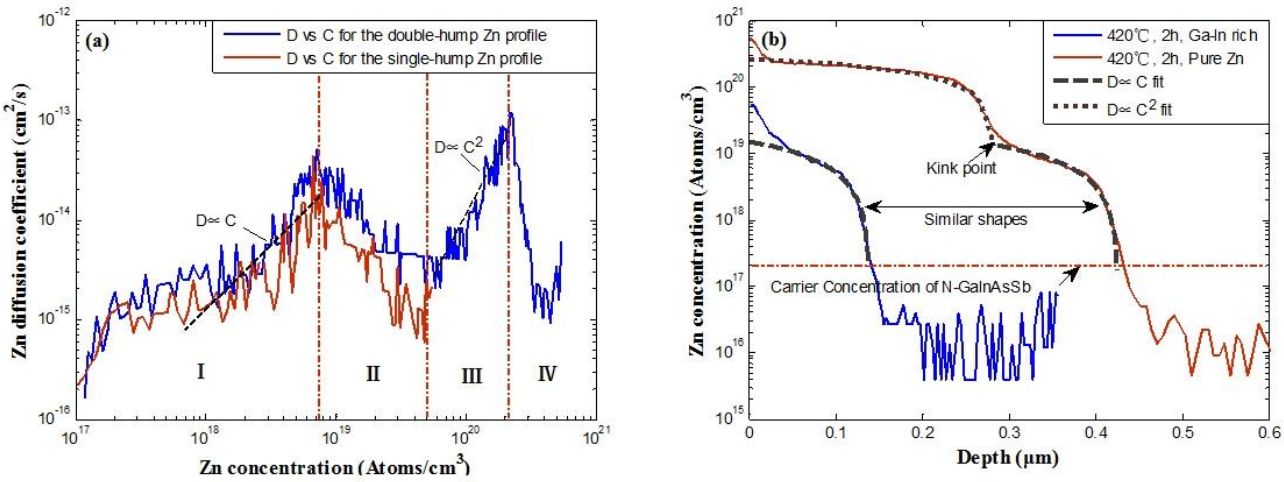

Fig. 4. (a) Zn diffusion coefficient as a function of concentration for typical single and double hump Zn profiles. (b) Simulations for the single and double-hump Zn profiles.

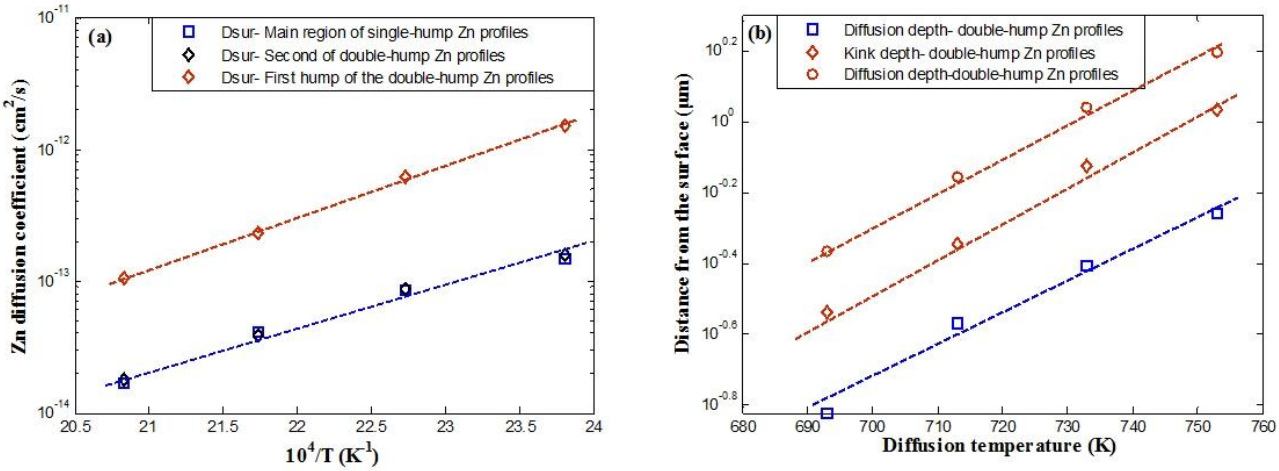

Fig. 5. (a) Arrhenius plot of D_{sur} fitted for simulating the single and double hump Zn profiles obtained at 420~480℃ for 2h. (b) Diffusion depth and kink depth for Zn profiles in Fig. 1a and 2a.

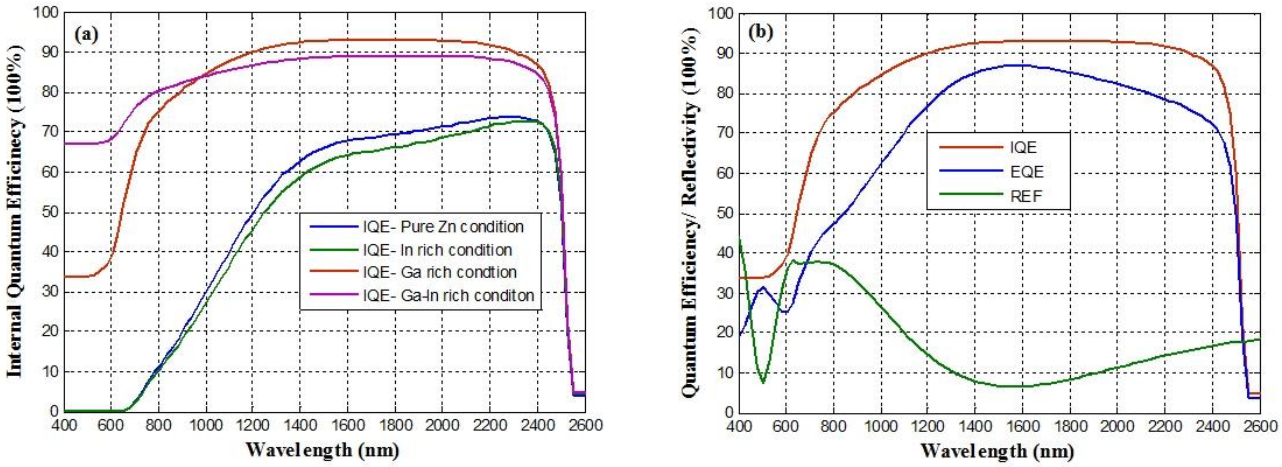

Fig. 6. (a) Simulated IQE of GaInAsSb cells with different Zn profiles at 300K. (b) Simulated IQE, EQE and REF of the cell obtained under Ga-rich condition.

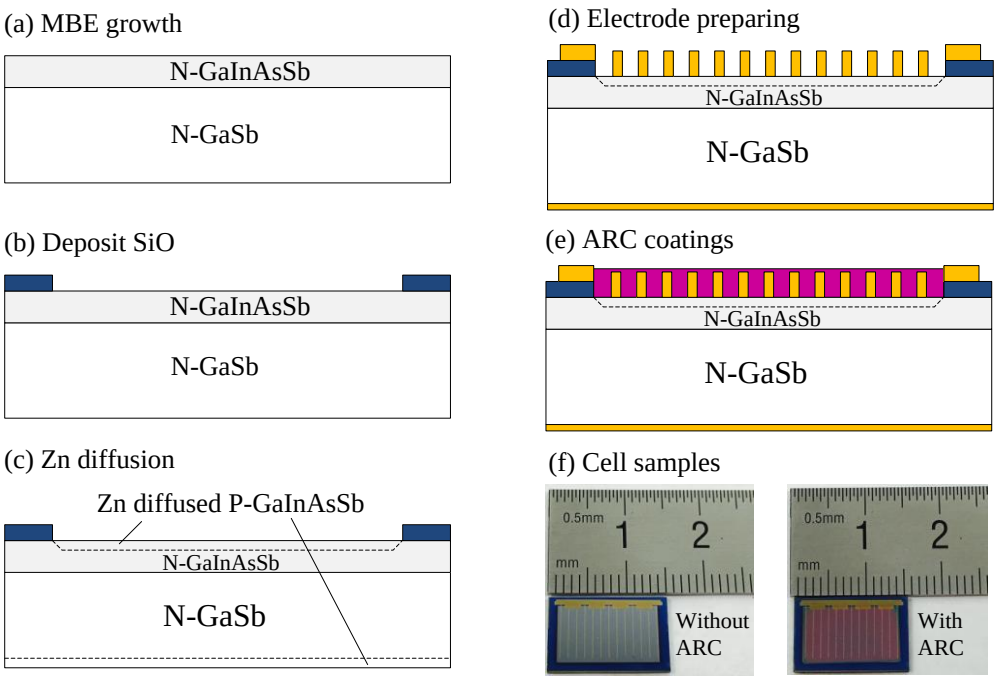

Fig. 7. GaInAsSb cell fabrication process using Zn diffusion method and cell samples.

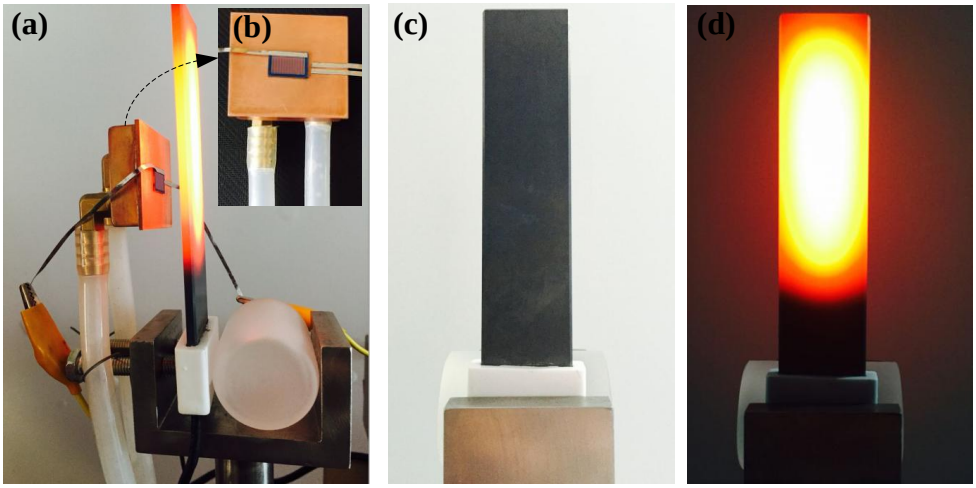

Fig. 8. A simple electrical heating TPV system used for output testing. (a) An overview; (b) A water cooling apparatus for cell mounting. (c) SiN ceramic emitter before and (d) after heated.

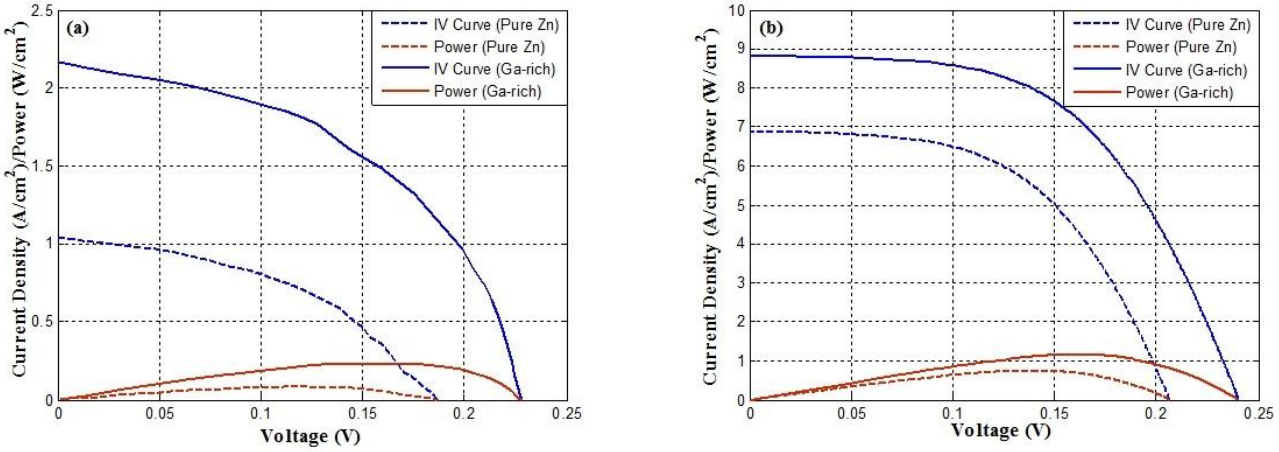

Fig. 9. The I-V curve and power output density of GaInAsSb cells under (a) 1055℃-SiN ceramic emitter and (b) 1055℃-given blackbody radiations.